Excited states in ^{129}I

D. Deleanu,[1,2] D. L. Balabanski,[3] Ts. Venkova,[3] D. Bucurescu,[1] N. Mărginean,[1] E. Ganioğlu,[4] Gh. Căta-Danil,[1,2] L. Atanasova,[3] I. Căta-Danil,[1] P. Detistov,[3] D. Filipescu,[1] D. Ghiţă,[1] T. Glodariu,[1] M. Ivaşcu,[1] R. Mărginean,[1] C. Mihai,[1] A. Negret,[1] S. Pascu,[1,5] T. Sava,[1] L. Stroe,[1] G. Suliman,[1] and N. V. Zamfir[1]

[1]*Horia Hulubei National Institute for Physics and Nuclear Engineering, 077125 Bucharest, Romania*

[2]*Physics Department, University Politehnica of Bucharest, R-060042 Romania*

[3]*Institute of Nuclear Research and Nuclear Energy, Bulgarian Academy of Sciences, Sofia 1784, Bulgaria*

[4]*Science Faculty, Physics Department, Istanbul University, 34134 Istanbul, Turkey*

[5]*Institut für Kernphysik, Universität zu Köln, Zülpicher Strasse 77, D-50937 Germany*

(Received 12 September 2012; revised manuscript received 4 December 2012; published 22 January 2013)

Excited states in ^{129}I were populated with the ^{124}Sn(^{7}Li,2n) reaction at 23 MeV. In-beam measurements of γ-ray coincidences were performed with an array of eight HPGe detectors and five $LaBr_3$(Ce) scintillation detectors. Based on the $\gamma\gamma$ coincidence data, a positive parity band structure built on the $7/2^+$ ground state was established and the $\pi g_{7/2}$ configuration at oblate deformation was assigned to it. The results are compared to interacting Boson-Fermion model (IBFM) and total Routhian surface (TRS) calculations.

DOI: 10.1103/PhysRevC.87.014329 PACS number(s): 21.10.−k, 21.60.Ev, 23.20.Lv, 27.60.+j

I. INTRODUCTION

The iodine nuclei have only three protons beyond the $Z = 50$ shell closure, yet the existence of a finite number of valence particles and holes causes the breaking of the spherical symmetry and induces deformation. Collective rotational bands associated with the $\pi g_{7/2}$, $\pi d_{5/2}$, and $\pi h_{11/2}$ orbitals were observed in the odd-A iodine nuclei up to $N = 74$ [1,2]. The low-lying states in the closed neutron-shell isotope ^{135}I are understood in terms of proton three-quasiparticle configurations [3–5]. In the neighboring ^{131,133}I isotopes, which were described within the shell model, three-quasiparticle states involving two neutron hole excitations were reported [6]. Thus, an interplay between collective and shell-model structures might be expected to occur in the ^{129}I.

Information about low-spin levels in ^{129}I were obtained from β^- decay of ^{129}Te [7], Coulomb excitation [8], and direct one-nucleon transfer (^{3}He,α) and (α, t) reactions [9]. Detailed comparisons of the experimental properties with calculations within different nuclear models were made, e.g., with the Alaga model [10], the three-particle-cluster-phonon coupling model [9], and the shell model in the S and D nucleon-pair approximation [11]. In addition, for the iodine isotopes with mass numbers up to $A = 127$, calculations with the interacting boson-fermion model-2 (IBFM-2) were performed [12].

Prior to this experiment nothing had been known about spin states higher than $11/2^-$ in this nucleus [13]. Here we report higher spin states in ^{129}I, populated in the ^{124}Sn(^{7}Li,2n) fusion-evaporation reaction at an incident energy of 23 MeV. A band structure built on the $\pi g_{7/2}$ ground state was established.

Total Routhian surface calculations for the $g_{7/2}$ quasiproton configuration in the odd-A ^{127,129,131}I nuclei demonstrate that these nuclei take oblate shapes. The experimental level scheme is compared to predictions of the interacting boson-fermion model-1 (IBFM-1).

II. EXPERIMENT, ANALYSIS AND RESULTS

Excited states in ^{129}I were populated in the ^{124}Sn(^{7}Li,2n) fusion-evaporation reaction. The experiment was done at the Bucharest Tandem Van de Graaff accelerator with both continuous and pulsed (1 ns wide pulses, 200 ns apart) ^{7}Li beams. An isotopically enriched 3.4 mg/cm^2 thick ^{124}Sn target on 13 mg/cm^2 gold backing was used.

The projectile energy was chosen on the basis of statistical model calculations using the CASCADE code [14]. These calculations indicate that the cross section of the ^{124}Sn(^{7}Li,2n)^{129}I reaction channel reaches a maximum value (∼2–3 mb) at around 23 MeV, but the cross section value remains significantly lower than the cross sections of the 4n and 3n (^{127,128}I) channels, which are about two orders of magnitude higher.

The γ rays emitted in the heavy-ion induced reactions were detected with a hybrid array of eight ∼50% relative efficiency high purity germanium (HPGe) detectors and five $LaBr_3$:Ce detectors. However, the statistics accumulated for the 2n reaction channel in this experiment was not sufficient to determine lifetimes in ^{129}I. The HPGe detectors were placed, with respect to the beam axis, as follows: five detectors in a ring at 143°, two at 90°, and one at 45°, while the $LaBr_3$:Ce scintillator detectors were placed bellow the target chamber at angles of ≈45° around an axis that is perpendicular to the beam axis. Neutrons were also detected with a one litter liquid NE223 scintillator detector placed at 25°. The data acquisition system was triggered either by two HPGe detectors, or by at least one HPGe detector and two $LaBr_3$:Ce detectors that fired in coincidence. While the γ coincidences between the HPGe detectors were used to construct the level scheme, the combination between HPGe and $LaBr_3$:Ce detectors served to look for level lifetimes longer than several tens of picoseconds, with the fast timing method described in Ref. [15].

In order to construct the level scheme the events were sorted into $\gamma\gamma$ and $\gamma\gamma\gamma$ coincidence matrices, respectively.

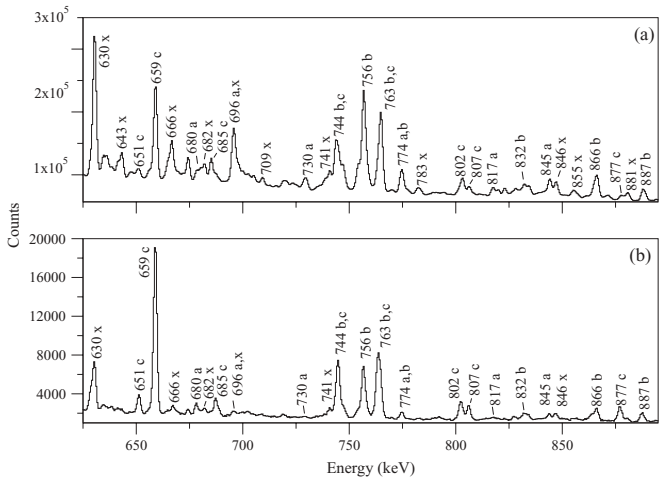

FIG. 1. Spectra showing the γ rays emitted in the ^{124}Sn(^{7}Li,xn) reaction at 23 MeV beam energy: (a) total projection of a $\gamma\gamma$-coincidence matrix, (b) total projection of a $\gamma\gamma$-coincidence matrix gated on neutrons. The γ rays are labeled by their energy a letter denoting the isotope (a for ^{129}I, b for ^{128}I, c for ^{127}I, and x for contaminants or not identified γ rays).

Sample of spectra representing the total projections of the $\gamma\gamma$ matrices obtained with pulsed beam data, or continuous beam data also gating on neutrons, are shown in Figs. 1(a) and 1(b), respectively. The gate on neutrons enhanced the $2n$, $3n$, and $4n$ channels. The γ rays previously assigned to ^{127,128}I [16,17] and the newly found in ^{128,129}I are labeled. Preliminary results on the newly established level scheme of ^{128}I were briefly reported in Ref. [18].

The main difficulty in the analysis was to exclude contributions from coincidences with overlapping γ rays. The 695.0 keV, $4^+ \rightarrow 2^+$ transition in ^{126}Te, which overlaps with the 695.7 keV transition in ^{129}I, made the construction of the level-scheme and the determination of the relative intensities rather difficult. The ^{126}Sb β^- decay feeds the 8^+, 6^+, and 4^+ states of ^{126}Te [19]. ^{126}Sb is produced in a deuteron transfer reaction ^{124}Sn(^{7}Li,αn), in which the ^{7}Li projectile, with energies near the Coulomb barrier, breaks in the Coulomb field of the target. In the spectrum shown in Fig. 1(a), the peaks at 695.0 keV and 666.3 keV, originating from β decay, are rather intense. The 695.7 keV peak, which corresponds to the $11/2^+ \rightarrow 7/2^+$ yrast transition of ^{129}I, cannot be distinguished from the 695.0 keV transition in ^{126}Te. The neutron gate condition rejected the γ-ray events from β decay [Fig. 1(b)]. However, the neutron detection efficiency was small and the neutron gated data were used only as a guideline. A significant decrease of $\sim$70% of the β-decay contribution was obtained when pulsed ^{7}Li beam was used.

Gamma rays were assigned to the ^{129}I isotope based on the coincidence data. Sample spectra showing the γ rays identified in ^{129}I are displayed in Fig. 2. Using an asymmetric $\gamma\gamma$ coincidence matrix, with the 143° detectors on one axis and the 90° detectors on the second axis, multipolarities of the transitions were also established, on the basis of DCO ratio values.

The ground state in ^{129}I had been previously determined to be $7/2^+$ based on β-decay studies [7]. The level scheme which was constructed as a result of our experiment is built above the $7/2^+$ ground state and is shown in Fig. 3. The first excited state in ^{129}I is the 28-keV $5/2^+$ level, which is also known from β decay [7]. The 729.6- and 695.7-keV γ rays that were observed in both β decay [7] and Coulomb excitation [8] experiments were identified in our experiment, too. The 844.9-, 817.2-, 556.7-, and 672.2-keV γ rays which were previously established in β decay, were observed as well, as shown in Fig. 3.

Relative γ-ray intensities were obtained with respect to the intensity of the 695.7 keV transition to the ground state. Since it is contaminated as explained above, special care had to be taken in order to obtain only its contribution from ^{129}I to this peak. The 666.3- and the 695.0-keV transitions from the β decay of ^{126}Sb have roughly the same intensity, ($I_{694.8}/I_{666.3} = 0.96(5)$ [19]). The radioactivity of the target was measured immediately after the experiment and the value we found for this ratio was 0.99(7), corresponding to the value expected from the decay of the 19 min isomer. Their peak areas in the total projections of the $\gamma\gamma$ matrices for pulsed and continuous beams were evaluated. With a pulsed beam, a $\approx$70% decrease of the 666.3 keV peak area was found. Thus, we could estimate the β-decay contamination in the total area of the 695 keV peak.

The DCO ratio values, $R_{\rm DCO}$, were obtained from the asymmetric $\gamma\gamma$ coincidence matrix, (with the 143° detectors

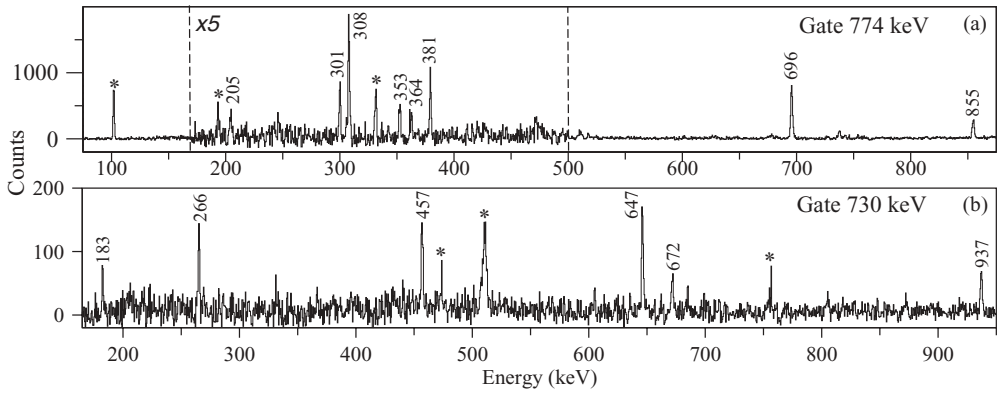

FIG. 2. Gated coincidence spectra showing the transitions assigned to ^{129}I. The γ rays are denoted by their energy. Peaks marked with star are identified as contaminant transitions from other nuclei.

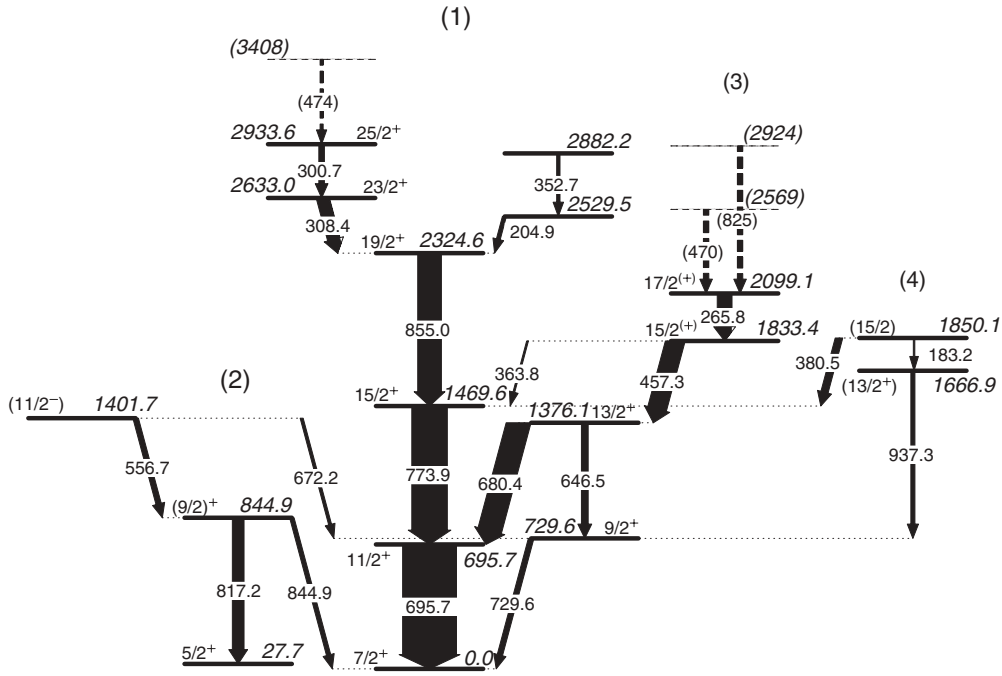

FIG. 3. Partial level scheme of ^{129}I as derived from the current study. The intensities of the γ transitions are proportional with the widths of the arrows and the corresponding values can be found in Table I. The structure of the level sequences denoted as (1), (2), (3), and (4) is discussed in the text.

on one axis and the 90° detectors on the second axis), according to the following definition:

$$R_{\mathrm{DCO}} = \frac{I(\gamma_1 \text{ at } 90^\circ; \gamma_2 \text{ at } 143^\circ)}{I(\gamma_1 \text{ at } 143^\circ; \gamma_2 \text{ at } 90^\circ)}.$$

If the gating transition, γ_1, is of a stretched quadrupole (Q) type, then the DCO ratio of γ_2 takes values of about 0.5 for a stretched dipole (D) transition and 1.0 for a stretched quadrupole (Q) transition and conversely, by gating on a D transition, the DCO ratios are about 1.0 or 2.0 for D or Q transition, respectively. These values were checked on known transitions of the strongly populated nucleus ^{127}I (the $4n$ reaction channel).

The adopted ENSDF spin values of all states that were known before are either not unique, or not certain [13]. Since the $2n$ channel was weakly populated, reasonably precise DCO data could be obtained from these data only for the strongest transitions. Precise transition multipolarity assignments require to gate on a transition with reasonably well known multipolarity. Therefore, we have re-examined the original works [7–9], where some preferences for the spin assignments are detailed.

The adopted ENSDF spin/parity assignment of the 695.7-keV state is $7/2^+, 9/2^+, 11/2^+$ [13], mainly based on the β-decay study [7] which combined the observed $\log(ft)$ value for the decay from a $11/2^-$ state with the γ decay towards the $7/2^+$ ground state. However, in the Coulomb excitation experiment [8], an a_2 angular distribution coefficient was measured for this transition. In Coulomb excitation states are excited mainly through stretched quadrupole $E2$ transitions. Since the value a_2 is clearly consistent only with the 11/2 spin value, we adopt a $11/2^+$ assignment for the 695.7 keV state. This result is also consistent with the systematics observed along the iodine isotopic chain.

Transition energies and multipolarities, relative γ-ray intensities, DCO ratios, as well as level energies, spins, and parities, (the tentative ones within parentheses), from this work are presented in Table I. Spin-parity assignments are based on previous assignments, the measured DCO ratio values, and isotope systematics as discussed below.

The cascade of three strong transitions [Fig. 3, sequence (1)] observed in this work above the ground state is very similar to the cascade of $E2$ transitions built on the first excited $7/2^+$ state of ^{127}I (denoted as band C in Ref. [20] and band B in Ref. [21]). Therefore, it is very likely that this is the positive parity yrast sequence in ^{129}I. The DCO ratio values for the 695.7-, 773.9-, and 855.0-keV transitions of this level sequence indicate indeed a cascade of transitions with the same multipolarity. Gating on any of these γ rays, DCO values close to unity are obtained for the others. Since we have adopted an $E2$ multipolarity for the lowest transition it becomes obvious that this is indeed a cascade of three $E2$ transitions from states with corresponding spins $11/2^+$, $15/2^+$, and $19/2^+$. This sequence continues with the 308.4-keV, stretched, quadrupole transition. Two more levels (the second tentative) were established above this level, spin and parity $I^\pi = 25/2^+$ was assigned to the first one, based on the measured DCO ratio of the 300.7-keV transition.

The reported DCO values in Table I demonstrate that the 680.4-keV transition is clearly of dipole type. The $E2$ multipolarity of the 646.5-keV transition results from a DCO value obtained when gating on the dipole-type transition connecting the 729.6-keV $9/2^+$ state with the ground state. This later transition has indeed a negative a_2 angular distribution

TABLE I. Gamma-ray transitions in ^{129}I, as found in the present work, associated with the level scheme from Fig. 3. The γ-ray transition intensities as well as their assignment (initial level energy, spin and parity of the initial and final level) are given in columns 2 to 5. Column 6 lists the γ-ray gates used for DCO analysis of the corresponding transition. In the last column the assigned multipolarity is listed.

E_γ (keV)	I_γ	Assignment			DCO gate[a]	$R_{\rm DCO}$	Assigned
		E_x (keV)	$J_i^{\pi_i}$	$J_f^{\pi_f}$	(E_γ/mult.)		multipol.
183.2(4)	3(1)	1850.1(5)	(15/2)	$(13/2^+)$			(D)
204.9(4)	7(2)	2529.5(6)		$19/2^+$			
265.8(3)	26(14)	2099.1(5)	$17/2^{(+)}$	$15/2^{(+)}$	695.7/Q	0.56(11)	$(M1/E2)$
					457.3/D	0.75(9)	$(M1/E2)$
300.7(3)	10(2)	2933.6(5)	$25/2^+$	$23/2^+$	695.7/Q	0.68(27)	$M1/E2$
					773.9/Q	0.60(28)	$M1/E2$
308.4(2)	23(3)	2633.0(5)	$23/2^+$	$19/2^+$	695.7/Q	1.10(34)	$E2$
					773.9/Q	1.05(21)	$E2$
352.7(4)	7(3)	2882.2(6)					
363.8(4)	3(1)	1833.4(4)	$15/2^{(+)}$	$15/2^+$			
380.5(3)	14(2)	1850.1(5)	(15/2)	$15/2^+$			
457.3(3)	35(4)	1833.4(4)	$15/2^{(+)}$	$13/2^+$	695.7/Q	0.55(13)	$(M1/E2)$
					729.6/D	1.11(51)	$(M1/E2)$
(470)		(2569)		$17/2^{(+)}$			
(474)		(3408)		$25/2^+$			
556.7(2)[b]	21(10)	1401.7(5)	$(11/2^-)$	$(9/2)^+$	844.9/(D)	0.47(25)	$(E1)$
					817.2/(Q)	0.58(10)	$(E1)$
646.5(3)	13(2)	1376.1(5)	$13/2^+$	$9/2^+$	729.6/D	2.62(79)	$E2$
672.2(3)[b]	5(2)	1401.7(5)	$(11/2^-)$	$9/2^+$			$(E1)$
680.4(2)	45(5)	1376.1(5)	$13/2^+$	$11/2^+$	695.7/Q	0.50(6)	$M1/E2$
					457.3/D	0.81(17)	$M1/E2$
695.7(2)[b]	100	695.7(2)	$11/2^+$	$7/2^+$	457.3/D	1.42(24)	$E2$
					773.9/Q	1.00(10)	$E2$
729.6(2)[b]	40(7)	729.6(2)	$9/2^+$	$7/2^+$			$M1/E2$
773.9(3)	66(6)	1469.6(4)	$15/2^+$	$11/2^+$	695.7/Q	1.04(13)	$E2$
817.2(2)[b]	22(2)	844.9(3)	$(9/2)^+$	$5/2^+$			$(E2)$
(825)		(2924)		$17/2^{(+)}$			
844.9(3)[b]	8(2)[c]	844.9(3)	$(9/2)^+$	$7/2^+$			$(M1/E2)$
855.0(2)	44(2)	2324.6(8)	$19/2^+$	$15/2^+$	695.7/Q	0.87(16)	$E2$
					773.9/Q	1.03(19)	$E2$
937.3(4)	8(2)	1666.9(4)	$(13/2^+)$	$9/2^+$	729.6/D	1.55(87)	$(E2)$

[a]Q and D denote the type of the gating transition, as a stretched quadrupole or dipole transition, respectively.
[b]Transitions assigned to ^{129}I in previous experiments [7,8].
[c]Intensity relative to the 817.2 keV branch, using the branching ratios from Ref. [13].

coefficient in the Coulomb excitation experiment [8], strongly supporting its $M1$ character. All these facts support a $13/2^+$ assignment for the 1376.1-keV state. The sequence of the 729.6-keV $9/2^+$ and the 1376.1-keV $13/2^+$ levels forms the unfavored sequence of the band-like structure built on the $7/2^+$ ground state, and it does not appear to continue with the 457.3-keV transition, which is of a dipole type. Thus, spin/parity of $I^\pi = 15/2^{(+)}$ were adopted for the 1833.4-keV level.

For the 844.9-keV state we prefer the assignment $(9/2)^+$ of Ref. [7], and the 817.2-keV transition may be assumed as the beginning of a quasi-band structure built on the $5/2^+$ state [Fig. 3, sequence (2)]. As this structure is not yrast, it is more weakly populated and higher-lying transitions of this sequence could not be found. The spin/parity assignment of $(9/2)^+$ for the 844.9-keV state is supported by the systematic features of lighter iodine isotopes and by the fact that this level decays via a strong γ ray of 844.9 keV to the $7/2^+$ ground state, a behavior also seen for the lighter isotopes, e.g., 687 keV in ^{127}I, 591 keV in ^{125}I and 533 keV in ^{123}I [1].

For the 1401.7-keV state spin/parity $I^\pi = (9/2^-, 11/2^-)$ is adopted [13]. Although the two DCO ratio values which we obtain for the 556.7-keV transition that de-excites this level do not readily indicate a dipole-type transition, we adopt $(11/2^-)$ for this level. Note, however, that the value obtained when gating on the 844.9-keV transition is consistent with a dipole type for the 556.7-keV transition if the 844.9-keV transition is a mixed dipole/quadrupole one. This spin/parity assignment is supported by the decays to the $(9/2)^+$ state of sequence (2) and to the $11/2^+$ state of sequence (1). It is in agreement with Ref. [7], and is consistent with the excitation energy systematics in the iodine isotopes shown in Fig. 4 [22–25].

The remaining spin assignments in Fig. 3 were made on the basis of the DCO ratio values from Table I. Several other

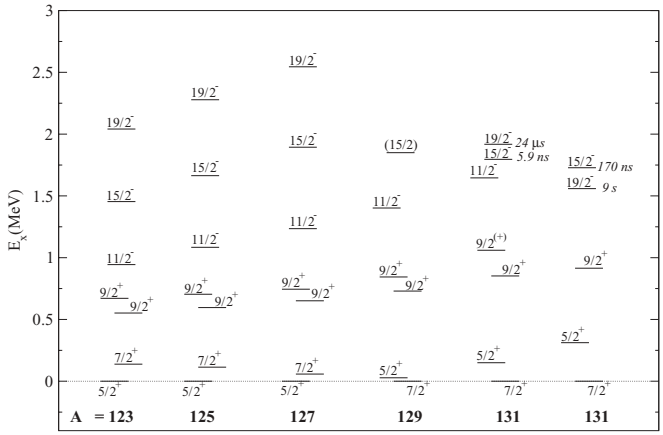

FIG. 4. Systematics of the $5/2^+_1$, $7/2^+_1$, $9/2^+_1$, $9/2^+_2$, $11/2^-_1$, $15/2^-_1$, and $19/2^-_1$ states in the odd $^{123-133}$I nuclei. Levels energies, spin, and parities are taken from Refs. [1,6,22–25,39,40].

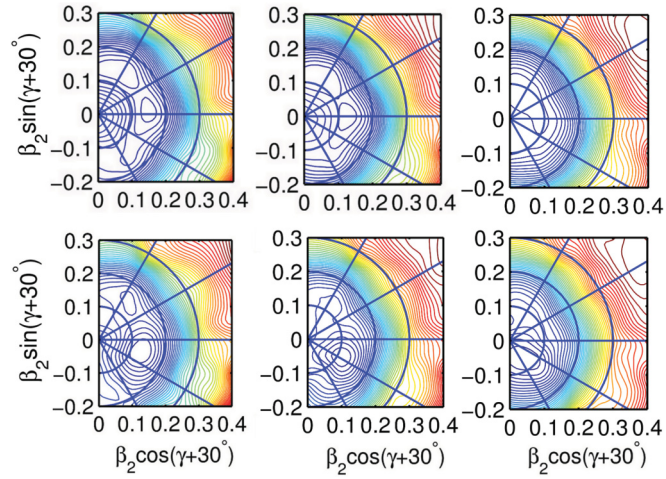

FIG. 5. (Color online) Total Routhian surfaces calculated at two rotational frequencies $\hbar\omega = 0.18$ MeV (up) and 0.3 MeV (down), for the $g_{7/2}$ structure in ^{127}I (left), ^{129}I (middle), and ^{131}I (right). The depth of the potential energy surfaces is given by the color coding, where blue (dark gray) shows the lowest energy and red (light gray) the highest. The energy difference between contour lines is 100 keV.

levels were established. Three relatively intense transitions (of 363.8 keV, 380.5 keV, and 457.3 keV) connect these states, denoted by (3) and (4) in Fig. 3, to the ground-state band. In addition, the 937.3-keV transition feeding the first $9/2^+$ level was observed in coincidence with a 183.2-keV γ ray, confirming the existence of the level at 1850.1 keV that decays to the $15/2^+$ state of sequence (1) via the 380.5-keV transition. For this level we tentatively adopt (15/2) based on its decay.

The relatively intense 265.8-keV γ ray, which feeds the $15/2^{(+)}$ level at 1833.4 keV indicates the presence of a level at 2099.1 keV. A couple of transitions were tentatively placed above this level. A spin of $17/2^{(+)}$ results for the 2099.1-keV level from the DCO analysis of the 265.8-keV transition (see Table I).

III. DISCUSSION AND CALCULATIONS

In ^{129}I, the positive parity sequence labeled (1) in Fig. 3 is built on the $7/2^+$ ground state, while the 817.2-keV transition may be considered as the beginning of another band structure, [labeled (2)], built on the excited $5/2^+$ state at 28 keV. Collective structures built on the $\pi g_{7/2}$ and $\pi d_{5/2}$ single-particle states had been previously observed in the lighter iodine isotopes [1,2] where the $I^\pi = 5/2^+$ and $I^\pi = 7/2^+$ states are the ground or the first excited state, (see Fig. 4). The electric quadrupole moments of these states were measured [26] as $Q_s(7/2^+) = -0.498(7)$ b and $Q_s(5/2^+) = -0.616(9)$ b, proving small oblate deformations.

Total Routhian surface (TRS) calculations for the odd $^{127-131}$I isotopes using Nilsson orbitals generated by the universal Woods-Saxon potential [27] are shown in Fig. 5. The total energy in the rotating frame (the Routhian) is minimized as a function of the deformation parameters β_2 and γ for each rotational frequency. A minimum of such a surface shows the favored deformation for a specific configuration of the nucleus at a specific rotational frequency [28,29]. Fig. 5 shows the TRS plots for ^{127,129,131}I calculated at two rotational frequencies $\hbar\omega = 0.18$ MeV and 0.3 MeV. At $\hbar\omega = 0.18$ MeV rotational frequency the TRSs predicts a $\beta_2 = 0.148$ and $\gamma \sim 26^\circ$ deformation for ^{127}I, a $\beta_2 = 0.128$ and $\gamma \sim 28^\circ$ for ^{129}I, and a $\beta_2 = 0.086$ and $\gamma \sim 29^\circ$ for ^{131}I, with increasing neutron number the β_2 deformation decreasing slightly, at higher frequencies the γ deformation driving the shape to triaxiality. The TRS calculations for the $7/2^+$ band in ^{129}I associated with one $g_{7/2}$ quasiproton configuration show that the oblate shape becomes dominant with increasing frequency and is consistent with the results of electric quadrupole moments measurements. This is associated with the gap created by the downsloping $5/2^+[413]$ and $7/2^+[413]$ proton orbitals, as displayed in Fig. 6.

Calculations within the framework of the interacting Boson-Fermion model-1 (IBFM-1) [30] were done. The calculation of level energies and electromagnetic transition probabilities were performed with the ODDA and PBEM [31] codes. In the IBFM-1 model, ^{129}I is considered as a ^{128}Te core described within the framework of the interacting boson approximation model-1 (IBA-1) [32], to which a fermion is coupled (in this case a proton particle) that can occupy the orbitals from the 50 to 82 major shell (for the positive parity states these are $g_{7/2}$, $d_{5/2}$, $s_{1/2}$, and $d_{3/2}$). The IBA-1 model parameters for the core are those from Ref. [33]. In the IBFM-1 Hamiltonian, besides the IBA-1 core Hamiltonian and the single-particle Hamiltonian, there is the boson-fermion interaction, for which three terms are of importance—a monopole-monopole, a quadrupole-quadrupole, and an exchange interaction [30].

In the semimicroscopic parametrization of the boson-fermion interaction [34], employed in the ODDA code, the three interaction terms are described by expressions that depend on the quasiparticle occupancies, multiplied by a strength parameter (named A_0, Γ_0, and Λ_0, respectively, in the ODDA code [31]). For the proton single-particle energies we have chosen the values of Reehal and Sorensen formulas [35], however, the energy difference between the $g_{7/2}$ and $d_{5/2}$ orbitals is reduced by 500 keV, as required in order to

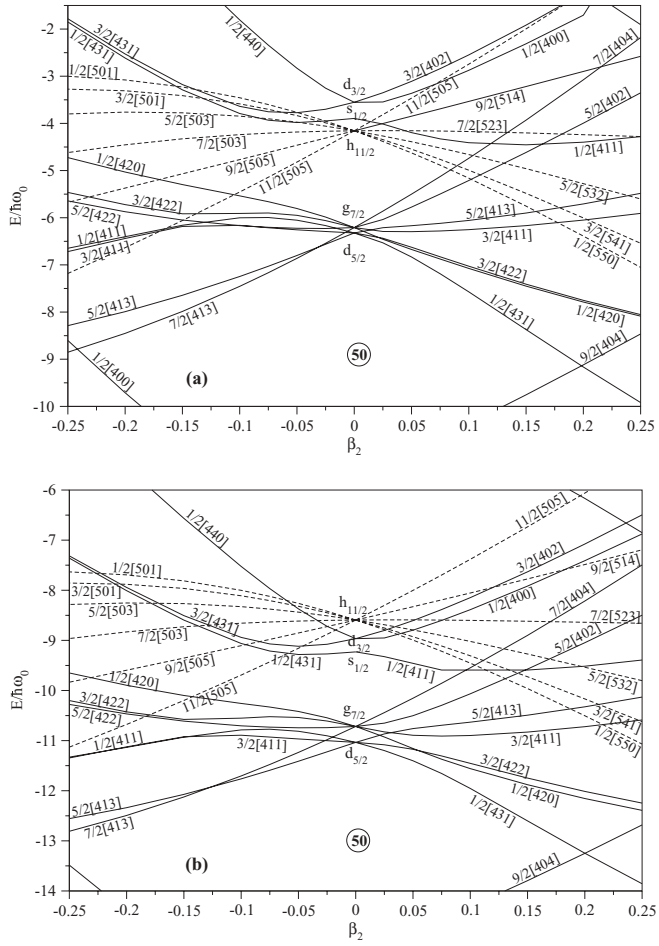

FIG. 6. Proton (a) and neutron (b) Nilsson orbitals calculated with the universal Woods-Saxon potential [27] for $\gamma = 0^\circ$. The orbits are labeled by the asymptotic quantum numbers $\Omega[Nn_z\Lambda]$. The energies are given in units $\hbar\omega_0$ ($=41A^{-1/3}$ MeV). Levels with even and odd parity are drawn with solid and dashed lines, respectively.

reproduce the low energy of the first excited $5/2^+$ level. The quasiparticle energies and occupancies were taken from a BCS calculation on these single particle energies. The three strength parameters used in these calculations, $A_0 = -0.10$ MeV, $\Gamma_0 = 0.17$ MeV, and $\Lambda_0 = 0.50$ MeV^2, were chosen in such a way as to generally reproduce both the excitation energy of the levels and their electromagnetic decays (branching ratios). Figure 7 shows a reasonable description of the low-spin levels, for which also a qualitative description of the electromagnetic decay branching ratios was obtained. The same parameters predict the higher-spin level scheme shown in Fig. 8. For the two band-like structures both the level energies and the electromagnetic decays are reasonably well described.

All calculated states are dominated by the lowest single-particle orbitals $g_{7/2}$ and $d_{5/2}$, the admixtures of the $s_{1/2}$ and $d_{3/2}$ orbitals in their structure being very small. The detailed properties of some of the low excited states (such as $1/2_1^+$, $3/2_1^+$, etc.) depend somewhat on the quasiparticle energies and occupancies chosen (for which we have not performed any extensive search), while the predictions for the higher spin

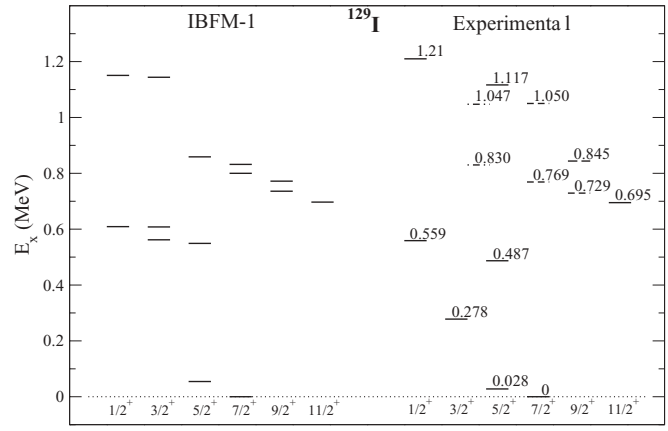

FIG. 7. Positive-parity levels of low spin and low excitation energy in ^{129}I [13]. Comparison of experimental levels with those calculated with IBFM-1. The experimental levels with tentative or ambiguous spin assignments are represented by dashed lines.

structures are rather stable for not too large variations of the quasiparticle level scheme and of the model parameters.

The yrast $7/2^+$, $11/2^+$, $15/2^+$, and $19/2^+$ states have a rather pure configuration with more than 98% contribution of the $\pi g_{7/2}$ orbital, and the $5/2_1^+$ state is almost 99% based on $\pi d_{5/2}$ orbital. The yrare states have a mixed $\pi g_{7/2}/d_{5/2}$ configuration: the $9/2^+$ and $13/2^+$ states from the "$d_{5/2}$" structure (Fig. 8) have the configurations $0.70d_{5/2} + 0.29g_{7/2}$ and $0.76d_{5/2} + 0.23g_{7/2}$, while the $9/2^+$ and $13/2^+$ states assigned as "$g_{7/2}$" have the configurations $0.29d_{5/2} + 0.70g_{7/2}$ and $0.23d_{5/2} + 0.76g_{7/2}$, respectively.

Therefore, we suggest that the positive parity structures (1) and (2) are built on slightly oblate shapes and have a mixed $\pi g_{7/2}/d_{5/2}$ configuration. The $7/2^+$ ground state and the associated band-like structure has mainly a $\pi g_{7/2}$ configuration with some admixture of the $\pi d_{5/2}$ configuration, while the $5/2^+$ state and the state above it have mainly a $\pi d_{5/2}$ configuration with some admixture of the $\pi g_{7/2}$ configuration. The $\pi g_{7/2}$- and $\pi d_{5/2}$-based structures are rather stable in

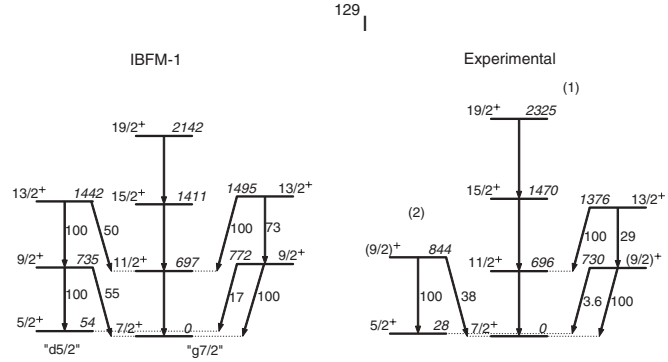

FIG. 8. Higher spin positive-parity levels assigned in the present measurements compared to predictions of the IBFM-1 calculations (same as those from Fig. 1). For the levels with more than one decaying γ ray, the transitions are labeled with their relative branching ratios, taken from [13] or the present work. The two calculated band-like structures are labeled by the dominating configuration.

excitation energy with increasing number of neutrons up to $N = 76$ (see Fig. 4).

A similar conclusion was reached for ^{123,125}I based on core-quasiparticle coupling model [36] or particle-rotor model (PRM) calculations [37], and for ^{127}I in the frame of the particle-triaxial-rotor model [38]. The three-particle cluster core coupling model investigation of Ref. [10] also reveals an important mixing between the $g_{7/2}$ and $d_{5/2}$ orbitals in the wave functions of the low-lying, low-spin states. In a recent paper Jia *et al.* [11] carried out systematic calculations on low-lying states in odd-A nuclei with $Z = 50$–58 and $N = 74$–90 using the nucleon pair approximation. The results for the excitation energies, the g factors, the electric quadrupole moments and the transition probabilities for the iodine isotopes in the vicinity of ^{129}I are in agreement with the results of the present experiment.

Throughout the chain of iodine isotopes, $11/2^-_1$ levels originating from the $\pi h_{11/2}$ orbital were established. The $11/2^-$ state rises in energy with an increasing number of neutrons and is observed up to ^{131}I (see Fig. 4). Decoupled sequences based on it were observed for the iodine nuclei with $N < 75$. It decays to the $(9/2)^+$ state of the $\pi d_{5/2}$-dominated sequence and to the $11/2^+$ state of the $\pi g_{7/2}$-dominated sequence. In ^{129}I we suggest $I^\pi = (11/2^-)$ for the 1401.7 keV level. Excited states built on it are not seen in ^{129}I, which might be due to the fact that other negative-parity states become yrast.

A number of three-quasiparticle ($3qp$) states and bands associated with them were observed in the lighter odd-mass iodine nuclei. These states lie at excitation energies between 2.0 and 3.0 MeV and have spins lower than 21/2. In ^{127}I the $\pi g_{7/2}$ band is crossed by a $23/2^+$ band which results from the breaking of a $h_{11/2}$ neutron pair and has the $\pi g_{7/2} \otimes (\nu h_{11/2})^2$ configuration [21]. The same structure we suggest for the $23/2^+$ state at 2633 keV in ^{129}I. The two observed transitions above might be the first members of this band.

A strongly populated $15/2^+$ state was established in ^{127}I at 2068.4 keV and a $3qp$ $(\pi g_{7/2}/d_{5/2})^3$ positive parity configuration was assigned to this state [21]. It decays mainly to the $13/2^+$ state of the $\pi g_{7/2}$ band, which is consistent with the configuration assignment. The 1833.4-keV $15/2^{(+)}$ level in ^{129}I has a similar decay pattern [labeled (3) in Fig. 3] and might have the same configuration.

In the ^{131,133}I isotopes, isomeric states having $I^\pi = 15/2^-$ [39,40] and $I^\pi = 19/2^-$ [6,41] were identified. The isomeric $15/2^-$ state has about the same energy in both isotopes. The isomeric $19/2^-$ state is lowered in energy when increasing the neutron number, becoming lower than the $15/2^-$ state in ^{133}I. The $15/2^-$ isomeric states were described as $\pi g_{7/2} \otimes \nu(d^{-1}_{3/2}h^{-1}_{11/2})_{5^-} 3qp$ states involving two neutron hole excitations. A state which decays in a similar way as the $15/2^-$ $3qp$ isomer in ^{131}I has been identified in the present experiment in ^{129}I at 1850.1 keV (see the systematics of Fig. 4 and Fig. 1 from Ref. [6]). Unfortunately, due to the low cross section of the $2n$ reaction channel one could not observe higher states feeding this level such as to be able to use the fast timing method [15] in order to evaluate its lifetime.

IV. CONCLUSIONS

Excited states in ^{129}I were established up to an excitation energy of about 3 MeV and tentative spin $I^\pi = (25/2^+)$. Positive-parity states are organized in band-like structures, which are suggested to have mixed $\pi g_{7/2}/d_{5/2}$ configurations dominated by either the $\pi g_{7/2}$ or the $\pi d_{5/2}$ orbital at oblate shapes. This conclusion is supported by nuclear moment measurements, nuclear structure systematics and TRS calculations. IBFM-1 calculations reproduce well the measured spectroscopic properties of the positive-parity states. The state at 1401.7 keV was tentatively assigned, on the basis of systematics, as the $(11/2^-)$ state originating from the $\pi h_{11/2}$ orbital.

Several $3qp$ states were observed in the neighboring odd-A iodine isotopes, involving either three quasiproton excitations (^{127}I), or two neutron hole excitations (^{131,133}I). It is interesting to find out whether such structures compete with oblate bands in ^{129}I. The sensitivity of our experiment has not been sufficient to unambiguously characterize the properties of such states. However, two states decaying to the $\pi g_{7/2}/d_{5/2}$ structure and assigned as $15/2^{(+)}$ and (15/2), respectively, have been observed and may constitute candidates for such excitations.

ACKNOWLEDGMENTS

Financial support from National Authority of the Scientific Research (ANCS), Romania, grants no. 24EU-ISOLDE and PN-09-37-01-05, IFA grants no. 6/2012-ISOLDE/PN II-Modul III and 460/PN II-Modul III, is duly acknowledged. The Bulgarian group acknowledges financial support from the National Science Fund, grants no. DID-02/16, DRNF-02/5, and DNTS-02/21. The authors thank the accelerator crew at Tandem, Bucharest, for their cooperation.

[1] R. E. Shroy, D. M. Gordon, M. Gai, D. B. Fossan, and A. K. Gaigalas, Phys. Rev. C **26**, 1089 (1982).
[2] M. Gai, D. M. Gordon, R. E. Shroy, D. B. Fossan, and A. K. Gaigalas, Phys. Rev. C **26**, 1101 (1982).
[3] C. T. Zhang *et al.*, Phys. Rev. Lett. **77**, 3743 (1996).
[4] S. K. Saha *et al.*, Phys. Rev. C **65**, 017302 (2001).
[5] C. Goodin *et al.*, Phys. Rev. C **78**, 044331 (2008).
[6] H. Watanabe *et al.*, Phys. Rev. C **79**, 064311 (2009).
[7] L. G. Mann *et al.*, Phys. Rev. C **14**, 1141 (1976).
[8] B. W. Renwick *et al.*, Nucl. Phys. A **208**, 574 (1973).
[9] A. S. de Toledo *et al.*, Nucl. Phys. A **320**, 309 (1979).
[10] A. S. de Toledo *et al.*, Phys. Rev. C **16**, 438 (1977).
[11] L. Y. Jia, H. Zhang, and Y. M. Zhao, Phys. Rev. C **76**, 054305 (2007).
[12] F. H. Al-Khudair, Phys. Rev. C **80**, 014306 (2009).
[13] Y. Tendow, Nucl. Data Sheets **77**, 631 (1996).
[14] F. Pühlhofer, Nucl. Phys. A **280**, 267 (1977).
[15] N. Marginean *et al.*, Eur. Phys. J. A **46**, 329 (2010).
[16] A. Hashizume *et al.*, Nucl. Data Sheets **112**, 1647 (2011).
[17] M. Kanbe and K. Kitao, Nucl. Data Sheets **94**, 227 (2001).

[18] D. Deleanu *et al.*, in *Proceedings of the International Conference on Nuclear Theory*, Vol. 29 (Heron Press, Sofia, Bulgaria, 2010), p. 32.
[19] J. Katakura *et al.*, Nucl. Data Sheets **97**, 765 (2002).
[20] Zhang Yu-Hu, M. A. Ying-Jun, Y. Sasaki, K. Yamada, H. Ohshima, S. Yokose, M. Ishizuka, T. Komatsubara, and K. Furuno, Chin. Phys. C **26**, 104 (2002).
[21] B. Ding *et al.*, Phys. Rev. C **85**, 044306 (2012).
[22] R. Goswami, B. Sethi, P. Banerjee, and R. K. Chattopadhyay, Phys. Rev. C **47**, 1013 (1993).
[23] H. Sharma, B. Sethi, R. Goswami, P. Banerjee, R. K. Bhandari, and J. Singh, Phys. Rev. C **59**, 2446 (1999).
[24] H. Sharma, B. Sethi, P. Banerjee, R. Goswami, R. K. Bhandari, and J. Singh, Phys. Rev. C **63**, 014313 (2000).
[25] D. Waard *et al.*, Phys. Lett. B **29**, 487 (1969).
[26] N. J. Stone, At. Data Nucl. Data Tables **90**, 75 (2005).
[27] W. Nazarewicz *et al.*, Nucl. Phys. A **435**, 397 (1985).
[28] R. Wyss *et al.*, Nucl. Phys. A **503**, 244 (1989).
[29] R. Wyss *et al.*, Nucl. Phys. A **511**, 324 (1990).
[30] F. Iachello and O. Scholten, Phys. Rev. Lett. **43**, 679 (1979).
[31] O. Scholten, computer codes ODDA and PBEM, KVI Internal Report No. 252 (1982).
[32] F. Iachello and A. Arima, *The Interacting Boson Model* (Cambridge University Press, Cambridge, 1987).
[33] D. Bucurescu *et al.*, Nucl. Phys. A **672**, 21 (2000).
[34] R. Bijker and A. E. L. Dieperink, Nucl. Phys. A **379**, 221 (1982); R. Bijker and O. Scholten, Phys. Rev. C **32**, 591 (1985).
[35] B. S. Reehal and R. A. Sorensen, Phys. Rev. C **2**, 819 (1970).
[36] L. G. Kostova *et al.*, Nucl. Phys. A **485**, 31 (1988).
[37] R. Goswami *et al.*, Z. Phys. A **352**, 395 (1995).
[38] H. C. Song *et al.*, Chin. Phys. Lett. **21**, 269 (2004).
[39] S. V. Jackson, W. B. Walters, and R. A. Meyer, Phys. Rev. C **11**, 1323 (1975).
[40] W. B. Walters, E. A. Henry, and R. A. Meyer, Phys. Rev. C **29**, 991 (1984).
[41] I. Bergstrom *et al.*, *Proceedings of the International Conference on Properties of Nuclides Far from the Region of β-Stability, CERN-70-30, Leysin, Switzerland*, 1970, Vol. 2, p. 1012.